Title

Multiscale Modeling of Inflammation-Induced Tumorigenesis Reveals Competing Oncogenic and Oncoprotective Roles for Inflammation.

Journal

Cancer research, 77(22)

ISSN

0008-5472

Authors

Guo, Yucheng
Nie, Qing
MacLean, Adam L
et al.

Publication Date

2017-11-01

DOI

10.1158/0008-5472.can-17-1662

Peer reviewed

Published OnlineFirst September 26, 2017; DOI: 10.1158/0008-5472.CAN-17-1662

Integrated Systems and Technologies: *Mathematical Oncology*

Cancer Research

Multiscale Modeling of Inflammation-Induced Tumorigenesis Reveals Competing Oncogenic and Oncoprotective Roles for Inflammation

Yucheng Guo[1], Qing Nie[2], Adam L. MacLean[2], Yanda Li[1], Jinzhi Lei[3], and Shao Li[1]

Abstract

Chronic inflammation is a serious risk factor for cancer; however, the routes from inflammation to cancer are poorly understood. On the basis of the processes implicated by frequently mutated genes associated with inflammation and cancer in three organs (stomach, colon, and liver) extracted from the Gene Expression Omnibus, The Cancer Genome Atlas, and Gene Ontology databases, we present a multiscale model of the long-term evolutionary dynamics leading from inflammation to tumorigenesis. The model incorporates cross-talk among interactions on several scales, including responses to DNA damage, gene mutation, cell-cycle behavior, population dynamics, inflammation, and metabolism-immune balance. Model simulations revealed two stages of inflammation-induced tumorigenesis: a precancerous state and tumorigenesis. The precancerous state was mainly caused by mutations in the cell proliferation pathway; the transition from the precancerous to tumorigenic states was induced by mutations in pathways associated with apoptosis, differentiation, and metabolism-immune balance. We identified opposing effects of inflammation on tumorigenesis. Mild inflammation removed cells with DNA damage through DNA damage-induced cell death, whereas severe inflammation accelerated accumulation of mutations and hence promoted tumorigenesis. These results provide insight into the evolutionary dynamics of inflammation-induced tumorigenesis and highlight the combinatorial effects of inflammation and metabolism-immune balance. This approach establishes methods for quantifying cancer risk, for the discovery of driver pathways in inflammation-induced tumorigenesis, and has direct relevance for early detection and prevention and development of new treatment regimes. *Cancer Res; 77(22); 6429–41. ©2017 AACR.*

Major Findings

Chronic inflammation is a serious risk factor for cancer; however, the routes from inflammation to cancer are poorly understood. A full understanding of these pathways is important for the prevention and treatment of inflammation-induced cancer. Here, based on the major processes implicated by frequently mutated genes associated with inflammation and cancer in three organs (stomach, colon, and liver) extracted from the Gene Expression Omnibus, The Cancer Genome Atlas, and Gene Ontology databases, we established a multiscale model from an evolutionary perspective that enables us to investigate the long-term processes implicated in inflammation-induced tumorigenesis. The model incorporates cross-talk between microscopic events, that is, DNA damage and gene mutations, and macroscopic events, that is, cell population dynamics driven by stem cell regeneration throughout an organism's lifetime. We identified driver pathways for tumorigenesis, demonstrated the opposing effects of inflammation, and revealed the importance of the interaction between inflammation and metabolism-immune balance in triggering tumorigenesis. This model provides a method for quantifying cancer risk based on the degree and duration of inflammation.

[1]MOE Key Laboratory of Bioinformatics and TCM-X Center/Bioinformatics Division, TNLIST, Department of Automation, Tsinghua University, Beijing, China. [2]Department of Mathematics, Department of Development and Cell Biology, Center for Mathematical and Computational Biology, University of California, Irvine, Irvine, California. [3]Zhou Pei-Yuan Center for Applied Mathematics, MOE Key Laboratory of Bioinformatics, Tsinghua University, Beijing, China.

Note: Supplementary data for this article are available at Cancer Research Online (http://cancerres.aacrjournals.org/).

Corresponding Authors: Shao Li, Department of Automation, Tsinghua University, Beijing 100084, China. Phone: 8610-6279-7035; Fax: 8610-6277-3552; E-mail: shaoli@tsinghua.edu.cn; and Jinzhi Lei, jzlei@tsinghua.edu.cn

doi: 10.1158/0008-5472.CAN-17-1662

Introduction

Epidemiologic data suggest that infection-driven chronic inflammation is linked to approximately 15% of the global cancer burden (1–4). Cancer risk increases strongly with the duration and extent of chronic inflammation (2, 5). As such, infection has gradually become accepted as a major driver of inflammation-induced tumorigenesis and hence a preventable cause of cancer (6). An understanding of the dynamic processes linking inflammation to tumorigenesis is crucial for the prevention and treatment of inflammation-induced cancer in general and for early diagnosis in particular.

The transition from inflammation to tumorigenesis is a prolonged process that results from the interplay between multiple

Published OnlineFirst September 26, 2017; DOI: 10.1158/0008-5472.CAN-17-1662

Quick Guide to Equations and Assumptions

Model Structure

We combined the major processes responsible for the progress from inflammation to tumorigenesis (Fig. 1A) to establish a multiscale model of stem cell regeneration in the inflammatory microenvironment (Fig. 1B; Supplementary Fig. S1).

In the model, the population dynamics arise from the dynamics of individual cells, each of which is based on a model of the cell-cycle dynamics, and the proliferation rate is dependent on the population size. We integrated the cell-cycle dynamics with individual heterogeneity due to DNA damage and pathway mutations (7). In addition, we modeled stochastically the effects of specific pathway mutations.

The model was implemented via single-cell–based model simulation, that is, we considered a system of multiple cells in which each cell undergoes the processes of proliferation, DNA damage response, gene mutation, apoptosis, or differentiation during each cell cycle. The probabilities of occurrence of each of these processes in an individual cell are inflammation-related and can be altered by gene mutations. The inflammatory microenvironment specifically affects the processes of proliferation, apoptosis, and the DNA damage response. After each cell cycle, the population size changes according to cell division, apoptosis, differentiation, or cell removal (due to metabolism-immune balance response) events (Supplementary Figs. S2–S6).

Major Assumptions

(i) Cells were classified into resting (G_0) or proliferating phases. During each cell cycle, a cell in the resting phase either irreversibly differentiates into a terminally differentiated cell or reenters the proliferating phase. A cell in the proliferating phase may undergo DNA damage and trigger a DNA damage response, resulting in either apoptosis or survival and continued cell-cycle progression. Proliferating cells can also exit the cell cycle through DNA damage–independent apoptosis. Each surviving cell divides into two daughter cells at the end of mitosis. Although we do not consider interactions between single cells explicitly, there is a dependence on the population size through the proliferation rate of each single cell.

(ii) Mutant cells in the resting cell pool can be cleared by the immune system due to the metabolism-immune balance (*MIB*) response. In the model, for each cell with two or more pathway mutations, there is a constant probability ($MIB > 0$) of being cleared in one cell cycle (Supplementary Eq. S4).

(iii) DNA damage triggers the processes of DNA damage repair and cell-cycle arrest or DNA damage–induced apoptosis if the damaged loci are not repaired. Nonrepaired cells can escape from damage-induced apoptosis and reenter the cell cycle such that over time, damage accumulates and can eventually induce functional gene mutations in the specific pathways of focus (Supplementary Section S1).

(iv) The inflammatory microenvironment affects the cell cycle and DNA damage in different ways, and cells can secrete a variety of signaling factors that perturb the inflammation level (Supplementary Section S1). To quantify the inflammation level, we applied the murine endoscopic index of colitis severity, which takes values from 0 to 15, as the inflammatory score (IS) to represent the grade of inflammation from zero to severe (Supplementary Section S1; Supplementary Fig. S2). Inflammation was included in the model through the relevant biological processes. Inflammation can promote cell proliferation, inhibit cell apoptosis, induce DNA damage, and repress DNA repair (Fig. 1B). Moreover, DNA damage can initiate the secretion of inflammatory cytokines such as IL6 that perturb the inflammatory microenvironment.

(v) To model gene mutation without the additional complexity of detailed gene-regulatory networks, we identified mutations by their effects on the relevant physiologic processes and represented them by changes in the model parameters (Fig. 1C; Supplementary Section S2). We considered mutations in eight pathways (Table 1; Supplementary Table S1). These pathways were subdivided into three types: (i) cell cycle: increasing the cell proliferation rate ($\Delta Prolif^+$); increasing the feedback strength to cell proliferation ($\Delta FSProlif^+$); decreasing the cell differentiation rate ($\Delta Diff^-$); or decreasing the cell apoptosis rate ($\Delta Apop^-$); (ii) DNA damage response: increasing the probability of DNA damage induction ($\Delta Damage^+$); decreasing the DNA damage repair efficiency ($\Delta Repair^-$); or increasing the probability of escaping apoptosis following unsuccessful DNA repair ($\Delta Escape^+$); (iii) MIB: here, we consider decreasing the rate of removal of mutant cells in the resting phase via MIB response (ΔMIB^-). The probability of a cell gaining one or more of the above mutations increases with the number of nonrepaired damaged loci. When a mutation event occurs, it is assigned equal probability of affecting any one of the above eight pathways, or resulting in no change to the model parameters.

Parameters

The proposed model is a general model for inflammation-induced tumorigenesis, and we focus mostly on its qualitative properties. For the calculation of cancer risk, we marked cancer initiation by a relative population (*RP*) value of $RP > 2$. See Supplementary Sec. S2 and Supplementary Tables S2 and S3 for details of the parameter values. For simulation, parameters were fit to the cumulative percentage of occurrence of colorectal cancer subsequent to a diagnosis of ulcerative colitis (Fig. 1D; Supplementary Table S4).

For details of the model formulation and implementation, see the Supplementary Material.

Published OnlineFirst September 26, 2017; DOI: 10.1158/0008-5472.CAN-17-1662

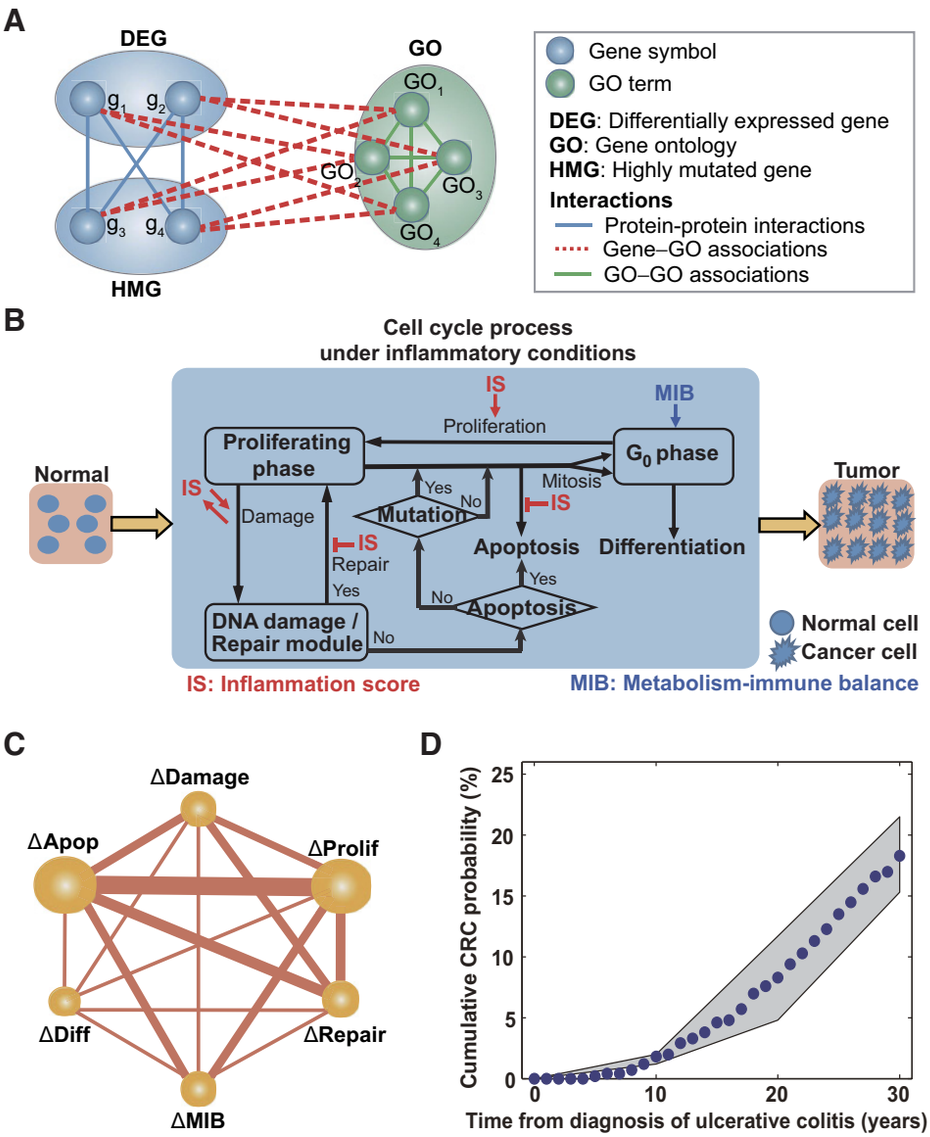

Figure 1.
Multiscale model of inflammation-induced tumorigenesis. **A,** Workflow identifying major pathways (by GO terms) associated with DEGs in different progression stages from chronic inflammation to cancer and HMGs based on the TCGA database. **B,** Illustration of the mathematical model framework. The model describes cell population dynamics with underlying single-cell–based attributes derived from three components: the cell cycle, DNA damage response, and inflammation. The black arrows represent the processes involved in stem cell regeneration; the red arrows show interactions with the inflammatory microenvironment, and the blue arrow represents the effect of the metabolism-immune balance (*MIB*) pathway that clears mutant cells to maintain G_0-phase homeostasis. **C,** Summary of pathway mutations observed in inflammation-induced tumorigenesis of colorectal cancer. Each node represents a pathway; the node size is proportional to the probability of finding mutations associated with that pathway, and the edge widths are proportional to the probability of finding a double mutation in a sample (see Supplementary Table S6 for a full list of genes). The mutations are defined as follows: $\Delta Apop^{-}$, cell apoptosis; $\Delta Damage^{+}$, DNA damage induction; $\Delta Prolif^{+}$, cell proliferation; $\Delta Repair^{-}$, DNA damage repair; ΔMIB^{-}, metabolism-immune balance response; $\Delta Diff^{-}$, cell differentiation. **D,** Cumulative risk of developing colorectal cancer following a diagnosis of ulcerative colitis. The blue points were obtained by model simulation; the gray region represents clinical data from ref. 28.

intracellular and extracellular processes. Multiple hallmarks are involved in the process, including proliferation abnormalities, genomic instability, metabolism-immune imbalance, reprogramming of the stromal environment, and aberrant transitions between epithelial and mesenchymal states. Inflammation is a cancer-promoting factor that contributes to the acquisition of most core cancer hallmarks (8). The major inflammatory cancer pathways converge on transcription factors STAT3 and NF-κB (1). However, inflammation can also act as a suppressor of tumorigenesis. The inflammasome can downregulate DNA repair and lead to cell death, a mechanism used by the immune system to eliminate cells with severe DNA damage (9, 10). Aspirin and other NSAIDs have received considerable interest as potential cancer chemopreventive agents (11–13). In addition, tumors themselves are actively involved in the modulation of inflammatory responses via manipulation of inflammatory factors and the immune system (14, 15). Despite these studies, the mechanisms by which inflammation promotes neoplastic transformation are incompletely understood, limiting our ability to translate knowledge of the pathways linking tumorigenesis and inflammation into therapeutic modalities. In addition, very few biomarkers of inflammation-induced tumorigenesis have been identified, thus

Table 1. Pathway mutations considered in the model

Symbol	Description
$\Delta Prolif$	Cell proliferation rate
$\Delta FSProlif$	Feedback strength on cell proliferation
$\Delta Diff$	Cell differentiation rate
$\Delta Apop$	Cell apoptosis rate
$\Delta Damage$	Probability of DNA damage induction
$\Delta Repair$	DNA damage repair efficiency
$\Delta Escape$	Probability of escaping from DNA damage-induced apoptosis
ΔMIB	Probability of removing mutant cells through metabolism-immune balance

Published OnlineFirst September 26, 2017; DOI: 10.1158/0008-5472.CAN-17-1662

limiting our ability to measure changes in cancer risk associated with chronic inflammation (16, 17).

Genomic data analysis and mathematical models have been valuable for deriving a detailed understanding of the somatic evolution of cancer (18–20). Today, single cancer cells can be analyzed in great detail at the molecular level, and tumor cell populations can be sampled extensively. Many computational models have been developed and used to describe aspects of cancer population dynamics (18, 21, 22). Agent-based models are often used to consider the more intricate spatiotemporal features of cancer, such as population structure and cellular interactions (23, 24). These modeling approaches have helped provide a detailed understanding of the mechanisms and processes implicated in cancer. Nevertheless, predictive modeling of the evolutionary dynamics of cancer is still a major challenge for computational biologists (19).

Despite the accumulation of molecular evidence linking cancer cells to the inflammatory microenvironment via multiple pathways, many of the mechanisms driving the transition from the inflammatory response to tumorigenesis remain elusive. Significant questions include: how do inflammatory insults promote the accumulation of DNA damage? How does inflammation play different roles in tumorigenesis? How can we predict the cancer risk associated with inflammatory diseases? What are the possible pathways from inflammation to tumorigenesis?

Here, by extrapolating from molecular details to pathway mechanisms, we established a hybrid multiscale model of inflammation-induced tumorigenesis from the perspective of evolutionary dynamics. The model considers the evolution of a system that combines individual cell behaviors with population dynamics through single-cell–based modeling, that is, the cells are heterogeneous with respect to the amount of DNA damage and the number of gene mutations they have experienced. In the model, we track individual cells undergoing, in each cell cycle, the processes of replication, DNA damage and DNA damage response, apoptosis, differentiation, and removal of mutant cells due to a metabolism-immune balance response. The probabilities of events related to inflammation can be altered by the occurrence of specific gene mutations. The model enables us to investigate the long-term process of inflammation-induced tumorigenesis. The model incorporates cross-talk between microscopic DNA damage response mechanisms and gene mutations in individual cells, and macroscopic cell population dynamics via stem cell–mediated tissue homeostasis and regeneration throughout life. We identify multiple driver pathways implicated in the transition from inflammation to tumorigenesis, demonstrate the opposing effects of inflammation on tumorigenesis in specific situations, and in particular highlight metabolism-immune balance as a key determinant for inflammation-induced tumorigenesis. Moreover, we provide a method by which specific cancer risk can be quantified on the basis of the degree and duration of inflammation.

Materials and Methods

Experimental data

Gene expression series (GSE4183, GSE2669, and GSE25097) were obtained from the Gene Expression Omnibus (GEO) database (http://www.ncbi.nlm.nih.gov/geo/). The Cancer Genome Atlas (TCGA) mutation datasets (colon and rectum adenocarcinoma, liver hepatocellular carcinoma, and stomach adenocarcinoma) were obtained from the UCSC Cancer Genomics Browser (https://genome-cancer.ucsc.edu/proj/site/hgHeatmap/). Gene Ontology (GO)–gene associations were obtained from the GO database (http://www.geneontology.org/gene-associations/). The procedures used for experimental data analysis are described in Supplementary Section S4.

Numerical scheme

In simulations, we initially set the IS, forbade mutations, and ran the model for 1,000 cycles so that the population size reached its stationary state (prior to mutation). We then allowed mutations to occur in subsequent simulations. For each set of parameters, we repeated the simulation process for 1,000 independent runs, thus simulating the evolutionary dynamics of many individuals.

One cell cycle in simulations was taken as 18 hours based on the proliferation rate of colonic epithelial cells (25). Hence, 1 year corresponds to 487 simulation cycles. For simplicity, we omitted the changes in the duration of the cell cycle that normally occur during the lifespan.

Statistical analysis

The time point $t = 0$ was chosen as the point at which gene mutations were initialized. As the cell population at $t = 0$ is dependent on the inflammation level, we reported the cell population at $t > 0$ as the relative population (RP), that is, the population size with respect to the population size at $t = 0$. The precancerous state was defined as the state in which $1.3 < RP < 1.6$, and tumorigenesis was assumed to occur when $RP > 1.6$ (Fig. 2A; Supplementary Fig. S7). For the calculation of cancer risk, we marked diagnosable cancer as having $RP > 2$.

The mutation frequency of a mutant type (whether harboring either single or double mutations) was given by the fraction F of cells possessing the given mutant type, formulated as

$$F(\text{mutation type}, t) = \frac{\text{Number of cells with mutation at time } t}{\text{Total number of cells at time } t.}$$

Results

Major processes responsible for the progression from inflammation to tumorigenesis

To investigate major processes responsible for the progression from inflammation to tumorigenesis, we combined data from three sources: GEO datasets for differentially expressed genes, TCGA database of mutant genes, and GO terms to identify the frequently mutated pathways that are associated with inflammation and cancer. The procedure is summarized in Fig. 1A and Supplementary Fig. S8 and described in detail in Supplementary Section S4. First, we explored the GEO datasets for three types of cancer (gastric, colorectal, and liver) to identify differentially expressed genes (DEG) that show statistically significant differences in expression between inflamed and healthy control samples and between cancer and control samples (Supplementary Fig. S8D–S8E; Supplementary Table S5). The numbers of DEGs associated with each cancer type are shown in Supplementary Fig. S8B. Next, for each cancer type, we examined the gene mutation data available from TCGA and obtained a set of highly mutated genes (HMG) whose mutations are linked to DEGs based on protein–protein interaction analysis (26). The numbers of HMGs are shown in Supplementary Fig. S8C and Supplementary Tables

Published OnlineFirst September 26, 2017; DOI: 10.1158/0008-5472.CAN-17-1662

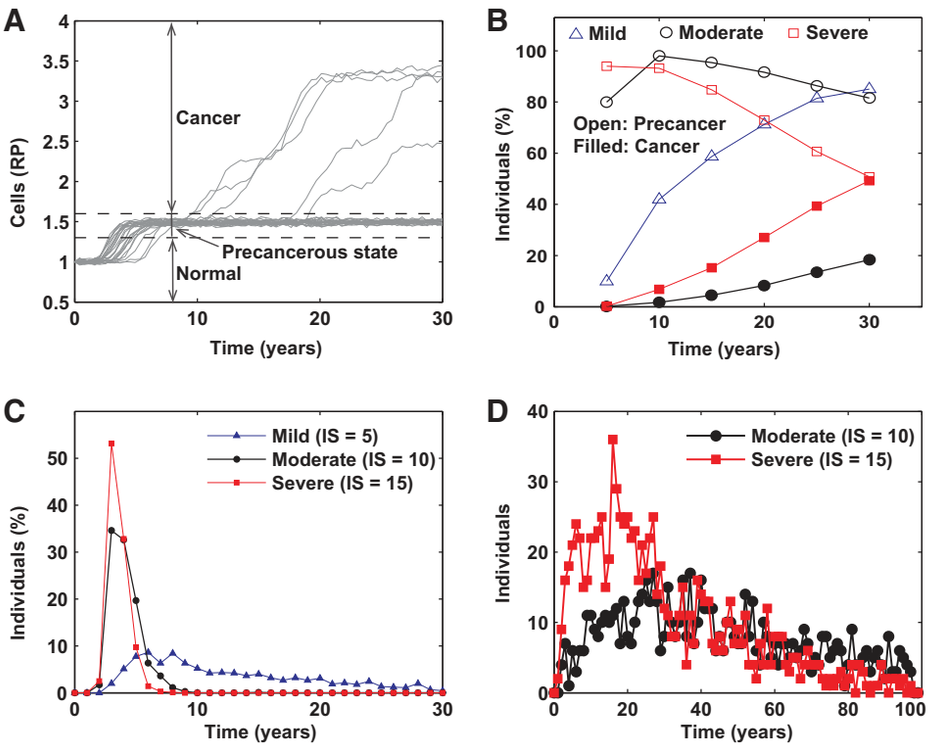

Figure 2.
Biphasic dynamics from inflammation to tumorigenesis. **A,** Evolutionary dynamics under moderate inflammation conditions ($IS = 10$). The relative population ($RP < 1.3$) denotes the population size relative to the initial population. Three stages can be defined by their dynamics: normal growth ($RP < 1.3$), the precancerous state ($1.3 < RP < 1.6$), and tumorigenesis ($RP > 1.6$). **B,** Percentage of cases (out of 1,000 independent runs) developing to the precancerous state (open circles) or to tumorigenesis (filled circles) at different time points after the onset of inflammation. The results for three inflammation conditions [mild ($IS = 5$, blue triangles), moderate ($IS = 10$, black circles), and severe ($IS = 15$, red squares)] are shown. No tumorigenesis was observed under mild inflammation conditions throughout the time course (15,000 cycles, 30 years). **C,** Distribution (fraction of individuals) of transition times from the normal to the precancerous state ($RP = 1.3$). **D,** Distribution (number of individuals) of times to the precancerous state under conditions of $IS = 10$ (black circles) and $IS = 15$ (red squares).

S6 and S7. To link the mutant genes with biological processes, we identified the GO terms that are implicated by at least one gene in the selected set of HMGs; this yielded 838 terms for gastric cancer, 493 terms for liver cancer, and 332 terms for colon cancer (Supplementary Table S8; Supplementary Fig. S8F). To eliminate redundancy in the obtained GO terms, we classified them into 20 categories based on key words in the GO names (Supplementary Tables S9 and S10; Supplementary Fig. S9).

Of the 20 GO category processes, nine were processes such as assembly, kinase activity, transcription, etc., that are associated with general transcription, translation, and protein–protein interaction processes (Supplementary Fig. S9). One process, migration, plays an important role in metastasis. The other 10 categories identified were apoptosis, proliferation, metabolism, cell cycle, senescence, DNA damage, telomerase, differentiation, immune response, and DNA repair. Dysregulation of these processes often results in abnormal cell growth; hence, they are major contributors to tumorigenesis. Analysis of the mutations implicated in these particular processes show that mutations in genes in the apoptosis and proliferation categories are highly cooccurrent in colorectal cancer (Fig. 1C; Supplementary Table S11). Moreover, frequent occurrence of double mutations in the processes of metabolism and apoptosis or proliferation, as well as double mutations in DNA damage and DNA damage repair processes, is observed.

In this study, we combined the major processes identified above with a model of cell-cycle dynamics to establish a hybrid multiscale model of stem cell regeneration in an inflammatory microenvironment (Fig. 1B). In the model, both senescence and telomere erosion result in permanent cell-cycle arrest or cell death (analogous to the cell flux that can occur either due to differentiation or to apoptosis); hence, we omitted these pathways for simplicity. For the structure and major assumptions of the model, see the Quick Guide to Equations and Assumptions.

Low- and high-grade inflammation have opposing effects on population size and accumulation of DNA damage

To investigate how the inflammatory microenvironment affects stem cell growth and the accumulation of DNA damage, we varied the *IS* from 0 to 15, forbade the occurrence of gene mutation, and ran simulations until the system reached a stationary state.

The stationary cell population depends nonlinearly on the *IS*: the population size increased with *IS* for $IS \leq 3$ and then decreased with *IS* for $IS > 3$, with an inflection point at $IS = 6$ (Supplementary Figs. S10 and S11). We further examined the numbers of cells that underwent apoptosis and mitosis at each cell cycle. There are two modes of apoptosis: independent of and induced by DNA damage. The rate of DNA damage–independent apoptosis decreased with *IS*, whereas that of DNA damage–induced apoptosis remained low for $IS \leq 3$ but increased with *IS* for $IS > 3$ (Supplementary Fig. S10C). Hence, the overall dependence of the apoptosis rate on *IS* showed two phases: a decrease during low-grade inflammation and an increase under conditions of higher grade inflammation. The mitosis rate was calculated as the ratio of the number of mitotic cells to the number of cells in the G_0 phase (before entering the proliferation phase) and shows a decrease with *IS* in low-grade inflammation and an increase with *IS* in higher grade inflammation (Supplementary Fig. S10B). Together, these results demonstrate the contrasting dependencies of population size on the inflammatory conditions: low-grade inflammation increases the cell population size due to a decreased rate of DNA damage–independent apoptosis, whereas higher

Published OnlineFirst September 26, 2017; DOI: 10.1158/0008-5472.CAN-17-1662

grade inflammation suppresses cell growth through an increasing rate of DNA damage–induced apoptosis.

To examine how inflammation promotes the accumulation of DNA damage, we analyzed the amount of DNA damage in each cell; from this, we obtained the distribution of cells and their corresponding number of nonrepaired DNA-damaged loci (Supplementary Fig. S10D). The results show that under normal conditions, nearly all cells were free of nonrepaired damaged loci. The percentage of cells with large numbers of damaged loci increased significantly when the inflammation became severe. The fraction of cells with accumulated DNA-damaged loci (more than 5 loci) increased linearly with *IS* for $IS > 6$ (Supplementary Fig. S10D, inset). We further examined the population dynamics and found that despite a decrease in the total cell population as the inflammation level increased from $IS = 3$ to $IS = 13$, the number of damaged cells increased with *IS* over this range (Supplementary Figs. S11 and S12). These results demonstrate that there are two phases in the accumulation of DNA-damaged loci in response to inflammation: low-grade inflammation usually does not increase the accumulation of DNA damage, but high-grade inflammation does promote the accumulation of DNA damage. These results are in agreement with experimental observations (27).

Biphasic dynamics from inflammation to tumorigenesis

To investigate the progression from inflammation to tumorigenesis, we initialized the system with moderate inflammation ($IS = 10$) and ran the model for a time period of 30 years (~15,000 cell cycles) to study the cell population dynamics. The overall cell population showed a biphasic increase following inflammatory disease, first to approximately $RP = 1.5$ (cell population relative to the homeostasis level) in 3 to 8 years, followed by a more rapid increase to a much higher level (up to $RP = 3$) in some individuals (Fig. 2A). We refer to the first phase, in which $1.3 < RP < 1.6$, as the precancerous state and to the second phase, in which $RP > 1.6$, as tumorigenesis.

To further examine the effects of inflammation on tumorigenesis, we compared simulations for mild ($IS = 5$), moderate ($IS = 10$), and severe ($IS = 15$) inflammation. In the case of mild inflammation, 90% of 1,000 independent individuals progressed to the precancerous state within 30 years, but no tumorigenesis was observed in this population. For both moderate and severe inflammation, the number of individuals in the precancerous state increased in the first few years, and this was followed by the onset of transitions from the precancerous state to tumorigenesis in later years (Fig. 2B). Particularly, when $IS = 10$, 176 of 1,000 individuals experienced tumorigenesis within 30 years, yielding a cancer rate of approximately 18%, comparable with clinical data (28).

Next, we analyzed the transition dynamics between normal tissue, the precancerous state, and tumorigenesis; these transitions are indicated in our model by the time points at which the *RP* reaches 1.3 and 1.6, respectively (Supplementary Fig. S7). For $IS = 5$, the timing of the transition from normal to precancerous state is distributed over a wide range, from 3 to 30 years, but when $IS = 10$ or $IS = 15$, the timing of this transition is more restricted, occurring between 3 and 8 years (Fig. 2C; Supplementary Fig. S13). These results indicate that moderate- to high-grade inflammation dramatically shortens the time required to reach the precancerous state.

The duration over which a precancerous state persists is crucial for tumorigenesis. We ran longer simulations for the conditions $IS = 10$ and $IS = 15$, extending the simulation time for up to 100 years after the onset of inflammation, and we examined the distribution of holding times between the precancerous state and cancer (Supplementary Fig. S7). Of 1,000 independent individuals, 755 developed tumorigenesis when $IS = 10$, and 957 developed tumorigenesis when $IS = 15$. The duration of the precancerous state was distributed over a wide range of values (0–100 years) under both conditions. Severe inflammation ($IS = 15$) substantially increased the probability density of existence of the precancerous state within the time window of 0 to 25 years, showing that, relative to moderate inflammation, high-grade inflammation promotes the transition from the precancerous state to tumorigenesis (Fig. 2D).

A single mutation in the cell-cycle pathway can give rise to a precancerous state

Gene mutations occur randomly in tissues at a rate on the order of 10^{-8} per base pair per generation (29). Very few of these mutations cause abnormal cell growth during later tissue development (30). When a mutation occurs in a stem cell, the mutant cell can either be removed or can survive to generate a colony of the mutant type (Supplementary Fig. S14). Here, we investigated the minimum number of mutations required to induce a precancerous state.

To study how the cell population dynamics respond to one mutation in a single pathway, we induced mutations of different types in 10% of the cells and examined the resulting cell population dynamics (Supplementary Fig. S15). The cell populations responded differently to mutations in different pathways (Fig. 3A). When the mutation occurred in the metabolism-immune balance pathway (ΔMIB^-), there were no significant changes in the numbers of mutant and wild-type cells (Fig. 3A; Supplementary Fig. S15E). When the mutation occurred in one of the pathways related to DNA damage, the total population size was maintained at the same level as before the mutation; however, the dynamics of the mutant cell population were affected by the type of mutation (Supplementary Fig. S15F–S15H). When the mutation increased DNA damage induction ($\Delta Damage^+$), the mutant cell population was quickly removed; when the mutation decreased DNA damage repair ($\Delta Repair^-$), the mutant cell population was slowly removed, and when the mutation increased the rate of cell escape from DNA damage–induced apoptosis ($\Delta Escape^+$), the mutant cell population was slowly expanded. When a mutation occurred in a cell-cycle pathway ($\Delta Prolif^+$, $\Delta FSProlif^+$, $\Delta Apop^-$, or $\Delta Diff^-$), the total number of cells increased to 130% to 150% of the level previous to the induction of mutation, indicative of the precancerous state. Moreover, the number of mutant cells increased, so that the mutant cells became dominant in each of these populations (Supplementary Fig. S15A–S15D). These results demonstrate the variety of possible responses to a single mutation. A mutation in either the metabolism-immune balance pathway or the DNA damage response pathway rarely results in abnormal cell growth, whereas a single mutation in one of the pathways that promote cell cycling leads to abnormal cell growth, accumulation of mutant cells, and the emergence of a precancerous state. Upon the emergence of a precancerous state, the surviving subpopulation of cells bearing the cell-cycle pathway mutation is potentially prone to further mutations that can lead to tumorigenesis. These steps are discussed in more detail below.

Published OnlineFirst September 26, 2017; DOI: 10.1158/0008-5472.CAN-17-1662

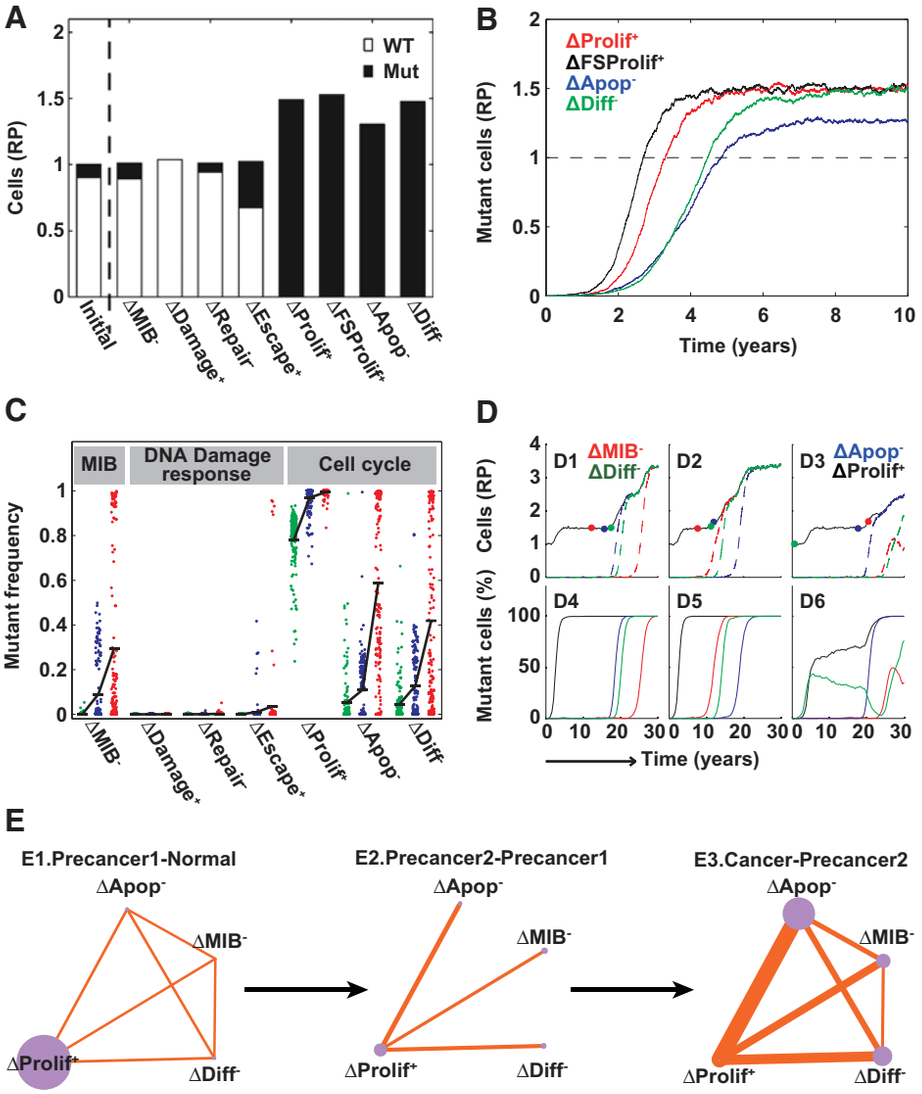

Figure 3.

Pathway mutations driving the transition from inflammation to tumorigenesis. **A,** Changes in the population size in response to a mutation in a single pathway. The bars show the relative populations of wild-type (white) and mutant cells (black). A single mutation was induced in 10% of the cells. The bar to the left of the dotted line shows the initial condition; the bars to the right of the dotted line show the relative populations 5 years after the induction of the indicated mutations. **B,** Dynamics of mutant cell populations after the induction of a mutation in a single cell. **C,** Distribution of mutation frequencies for different pathways at each of the three time points: $RP = 1.3$ (green), 1.6 (blue), and 2.0 (red; see Materials and Methods for details). A total of 153 individuals who developed tumors were analyzed; each point represents an individual. The black bars show the mean values in each case. **D,** Evolutionary dynamics from three sample runs (columns). The top panels (D1–D3) show the population dynamics of all cells (black solid line) and of double-mutant cells: $\Delta Prolif^{+}\Delta MIB^{-}$ (red dashed line), $\Delta Prolif^{+}\Delta Apop^{-}$ (blue dashed line), and $\Delta Prolif^{+}\Delta Diff^{-}$ (green dashed line). The bottom panels (D4–D6) show the percentages of mutant cells that have undergone specific mutations: $\Delta Prolif^{+}$ (black), ΔMIB^{-} (red), $\Delta Apop^{-}$ (blue), and $\Delta Diff^{-}$ (green). **E,** Summary of the double mutations present at the three time points. Each node represents a mutation type, and its size is proportional to the corresponding mutant frequency; each edge connecting two nodes represents a double mutation, and its width is proportional to the frequency of the double mutation (see Supplementary Fig. S16 for details).

As mutations in the cell-cycle pathway result in abnormal cell growth, we further studied the population dynamics in response to a mutation in one of the cell-cycle pathways in a single cell (rather than in a subset of 10% of the cells). In each case, the mutant cell is either eliminated from the population or survives to form a subpopulation of mutant cells (Supplementary Fig. S14). In our simulations, approximately 20% of individuals harbor mutant cells one year after the induction of the mutation (Supplementary Fig. S14). In these individuals, the number of mutant cells increases in a sigmoidal fashion, approaching a new stationary state approximately 6 years after the occurrence of the mutation (Fig. 3B). Mutations in the proliferation pathways ($\Delta Prolif^{+}$ or $\Delta FSProlif^{+}$) cause more rapid accumulation of mutant cells than mutation in the apoptosis ($\Delta Apop^{-}$) or differentiation ($\Delta Diff^{-}$) pathways (see also Fig. 3B). These results confirm that one mutation in a cell cycle–related process in a single cell is sufficient to produce a significant subclone or even to replace the entire population of nonmutant cells and that the accumulation of mutant cells occurs more rapidly when the mutation is in a proliferation pathway. These findings are consistent with cancer genomics data showing that mutations in proliferation pathways are among the most frequently observed types of mutations in several cancer types (Supplementary Fig. S9).

Double mutations provide early markers for the transition from the precancerous state to tumorigenesis

To investigate the mutations responsible for the transition from the precancerous state to tumorigenesis, we tracked the mutation routes followed by individual cells within populations that developed into cancer over a 30-year period following the onset of inflammation. Hereafter, as mutations of both the $\Delta Prolif^{+}$ and $\Delta FSProlif^{+}$ types result in an increase in the proliferation rate, we merged them into a single type, $\Delta Prolif^{+}$. We calculated the frequency of each mutant type for single mutations and for the combination of double mutations at three time points: $RP = 1.3$, 1.6, and 2.0 (Materials and Methods). The three time points correspond to the stages of early precancerous state,

Published OnlineFirst September 26, 2017; DOI: 10.1158/0008-5472.CAN-17-1662

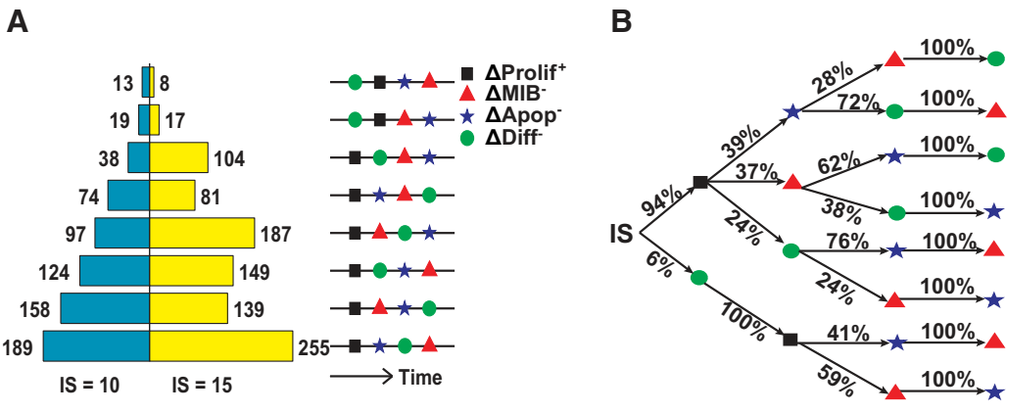

Figure 4.

Multiple routes to tumorigenesis. **A,** Bars showing the frequency per 1,000 individuals of each mutational sequence that led to tumorigenesis for $IS = 10$ (left) and $IS = 15$ (right). **B,** Illustration of the multiple routes from inflammation to tumorigenesis as a random process of pathway mutations. The numbers above the arrows show the probabilities of mutation in an individual with four accumulative mutations considered ($IS = 10$).

transition from the precancerous state to tumorigenesis, and full tumorigenesis.

Mutations in the proliferation pathway ($\Delta Prolif^+$) were highly occurrent (80%) in the early precancerous state (Fig. 3C). We also note the emergence of mutations in the apoptosis ($\Delta Apop^-$) and differentiation ($\Delta Diff^-$) pathways, but other mutations were rarely present in the early precancerous state. These findings are in agreement with the results of the previous analysis, which showed that a single mutation in the proliferation pathway could give rise to the precancerous state and that single mutations in the pathways of metabolism-immune balance or DNA damage response were not alone sufficient to induce abnormal cell growth.

During the progression from the precancerous state to tumorigenesis, a significant increase in the number of mutations in the pathways of metabolism-immune balance (ΔMIB^-), cell apoptosis ($\Delta Apop^-$), and cell differentiation ($\Delta Diff^-$) occurred. Nevertheless, the occurrence of mutations in DNA damage response pathways remained low except for a slight increase in mutations in the pathway of escape from DNA damage–induced apoptosis ($\Delta Escape^+$) during tumorigenesis (Fig. 3C).

We next examined the frequencies of double mutations. The double mutation rates of any type of mutation are low in the early precancerous state (Fig. 3E). At the transition stage from the precancerous state to tumorigenesis, the occurrence of double mutations in $\Delta Prolif^+$ plus either $\Delta Apop^-$, $\Delta Diff^-$, or ΔMIB^- increases, and it further increases at the stage of tumorigenesis (Fig. 3E, Supplementary Fig. S16). These results highlight the significant effects of mutations in pathways related to proliferation, cell apoptosis, differentiation, and metabolism-immune balance in the progression toward tumorigenesis.

To study how the above mutations work in coordination to trigger transition dynamics, we explored the population dynamics of three typical individuals (Fig. 3D). In these three individuals, mutations in the proliferation pathway occurred after inflammation to induce a precancerous state. The precancerous state persisted until a mutation in either ΔMIB^-, $\Delta Apop^-$, or $\Delta Diff^-$ occurred, at which point the transition to tumorigenesis occurred, along with an increase in the number of cells with double mutations (Fig. 3D). This result suggests that the double mutations $\Delta Prolif^+\Delta Apop^-$, $\Delta Prolif^+\Delta Diff^-$, and $\Delta Prolif^+\Delta MIB^-$ may serve as possible early biomarkers for an increased risk of transition from the precancerous state to tumorigenesis.

Multiple routes exist from inflammation to tumorigenesis

We have seen that the four mutations $\Delta Prolif^+$, ΔMIB^-, $\Delta Apop^-$, and $\Delta Diff^-$ occur frequently during tumorigenesis (Fig. 4A). To investigate the occurrence of particular sequences of combinations of these mutations, we characterized each individual run by ordering the four mutations in accordance with the criterion that 50% of all cells posses the given mutation (Supplementary Fig. S17). Thus, for each run, we have an ordered sequence of the four mutations. We summarized those sequences that developed to tumorigenesis (712/1,000 individual runs) within 100 years after the induction of moderate inflammation ($IS = 10$) and severe inflammation ($IS = 15$). The results showed that a mutation in the proliferation pathway, $\Delta Prolif^+$, was very likely to be the earliest event among these mutations, occurring first in more than 94% of cases; a mutation in the differentiation pathway, $\Delta Diff^-$, was the earliest event in the other tumorigenesis cases (Fig. 4A). The most frequent mutational sequence under both $IS = 10$ and $IS = 15$ was $\Delta Prolif^+ \rightarrow \Delta Apop^- \rightarrow \Delta Diff^- \rightarrow \Delta MIB^-$; this sequence occurred in more than 25% of the runs that led to tumorigenesis (Fig. 4A).

Following the occurrence of $\Delta Prolif^+$, the probability of the second mutation being any of the other three types was fairly similar; however, the third mutational step, $\Delta Apop^-$, was significantly less likely to occur last, that is, $\Delta Apop^-$ was more likely than $\Delta Diff^-$ or ΔMIB^- to occur as the second or the third mutation. From the sequence of pathway mutations in each individual, we determined the different possible routes to inflammation-induced tumorigenesis. These are represented as a progression tree in which the probability of occurrence of each mutation is dependent on the specific pathway (Fig. 4B). This progression tree allows quantification of the degree of progression for each tumor, for example, the expected waiting time for the specific mutational pattern to accumulate (31, 32). Hence, this progression model is of value in the prediction of evolutionary biomarkers of tumor evolution (19, 33).

Published OnlineFirst September 26, 2017; DOI: 10.1158/0008-5472.CAN-17-1662

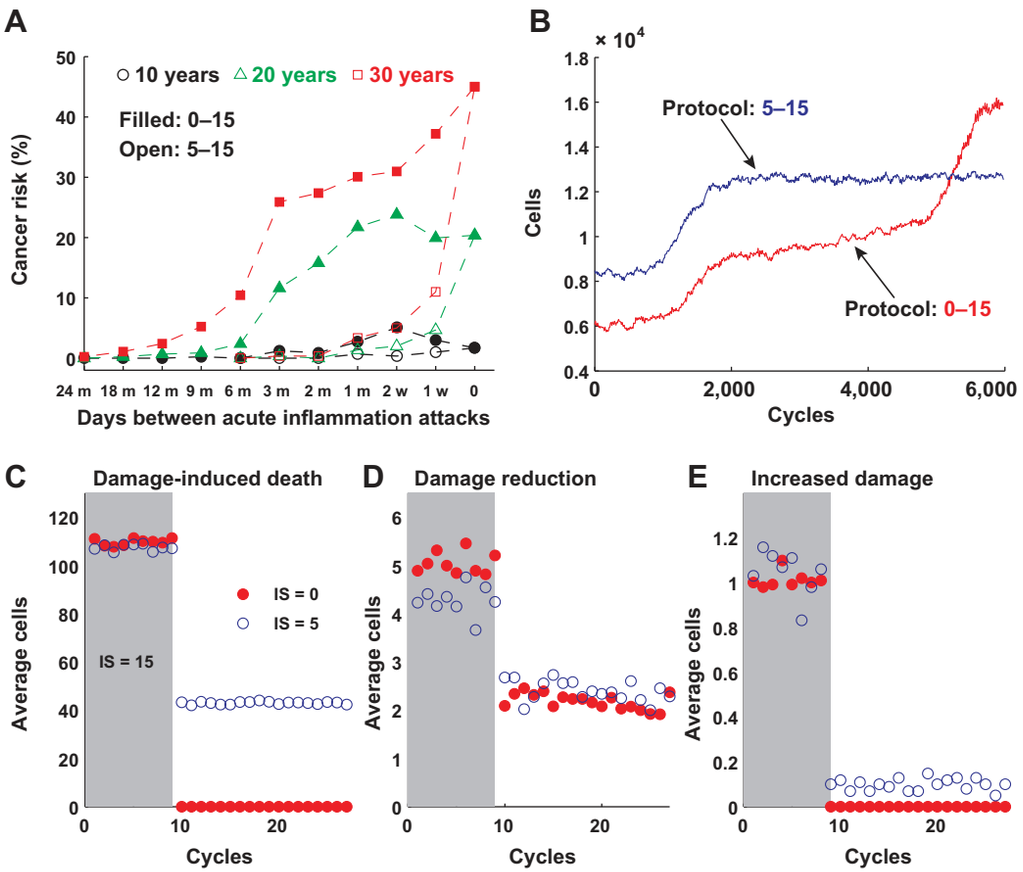

Figure 5.

The effects of periodic acute inflammation and cancer risk. **A,** Cancer risk under two protocols: 0–15 (filled circles) and 5–15 (open circles) for periodic acute inflammation attacks (Supplementary Table S12). In each period, acute inflammation ($IS = 15$) was induced for 1 week (9 cell cycles), followed by either zero ($IS = 0$, protocol 0–15) or low-grade inflammation ($IS = 5$, protocol 5–15) for a duration ranging from 1 week to 24 months. The markers show the occurrence of tumorigenesis at the three time points: 10 years (black), 20 years (green), or 30 years (red). A gap duration of 0 implies sustained acute inflammation. **B,** Evolutionary dynamics for each type of periodic acute inflammation attacks, both with a gap duration of 2 weeks. **C,** Average number of cells that underwent DNA damage–induced cell death at each cell cycle. **D,** Average number of cells with a reduction in the number of DNA-damaged loci at each cell cycle. **E,** Average number of cells with an increase in the number of DNA-damaged loci at each cell cycle. The average cell numbers in **C–E** were calculated from the trajectory of **B** from cycles 2,000 to 5,000, which correspond to the precancerous stage.

During periodic acute inflammation, mild inflammation between attacks protects against tumorigenesis

We have seen that severe chronic inflammation significantly increases cancer risk, whereas mild chronic inflammation can induce the precancerous state but does not show a clear correlation with cancer risk. Clinically, many patients with chronic inflammation show sustained mild chronic inflammation along with occasional or repeated acute inflammation attacks. We thus investigated how the occurrence of repeated episodes of acute inflammation might affect cancer risk. To this end, we considered individuals who were inflammation free ($IS = 0$) or who exhibited mild inflammation ($IS = 5$) and repeatedly induced 1 week (9 cell cycles) of acute inflammation ($IS = 15$), with the time period between acute inflammation attacks ranging from 1 week to 24 months. The two protocols corresponding to no inflammation and mild inflammation were termed protocol 0–15 and protocol 5–15, respectively (Supplementary Figs. S18 and S19).

We calculated the cancer risk based on simulation of 1,000 independent individuals at 10, 20, and 30 years after the onset of inflammation (Fig. 5A; Supplementary Table S12). In all cases, when the period between attacks was sufficiently long, the cancer risk was equivalent to that of individuals who experienced no acute inflammation attacks. Under both protocols, the cancer risk increased with the frequency of acute inflammation attacks except for a slight decrease under the 0–15 protocol when the time between acute inflammation attacks was less than 2 weeks. These results demonstrate that frequent acute inflammation attacks increase the risk of cancer.

Surprisingly, the simulations showed that under conditions of mild chronic inflammation (protocol 5–15), the cancer risk was much lower than when the intervals between acute inflammation attacks were inflammation free (protocol 0—15; Fig. 5A; Supplementary Figs. S18 and S19). For example, when we consider the cancer risk over 20 years (Fig. 5A, green), the risk associated with inflammation-free periods was much higher than the risk

Published OnlineFirst September 26, 2017; DOI: 10.1158/0008-5472.CAN-17-1662

associated with mild inflammation periods between acute inflammation attacks, when the time between acute inflammation attacks ranged from 1 week to 6 months. This difference was mainly due to the persistence of the precancerous state under protocol 5–15 (Fig. 5B). This counterintuitive result suggests that mild inflammation might play a dramatically different, protective, role compared with high-grade inflammation.

Acute inflammation promotes the accumulation of DNA damage (Supplementary Fig. S10D); however, based on our previous findings, we wished to assess whether the presence of mild inflammation between acute inflammation attacks attenuates the accumulation of damaged cells. We examined the precancerous state at the single-cell level and classified the cells according to their fates during the cycle: removal by DNA damage–induced death; reduction in DNA damage (fewer DNA-damaged loci remaining after completion of the cell cycle); or increase in DNA damage (more DNA-damaged loci remaining after completion of the cell cycle). The average cell numbers at each cell cycle during and after an acute inflammation attack are shown in Fig. 5C–E. These results indicate that mild inflammation can attenuate the accumulation of DNA damage by removing damaged cells via the pathway of damage-induced cell death.

The number of cells that undergo damage-induced cell death between acute inflammation attacks is larger under $IS = 5$ than under $IS = 0$ (Fig. 5C). The numbers of cells with reduced or increased levels of damage do not differ under the two protocols (Fig. 5D and E). These results intriguingly suggest opposing effects of inflammation on cancer risk (34): sustained high-grade inflammation tends to promote tumorigenesis due to the accumulation of DNA-damaged loci, whereas mild inflammation (even with interspersed acute inflammation attacks) tends to inhibit tumorigenesis by removing damaged cells.

Discussion and Conclusions

Chronic inflammation can increase cancer risk, but quantification of the mechanisms by which this occurs has been lacking. We have established a multiscale model of the evolutionary processes of inflammation-induced tumorigenesis. The model was developed to describe the major biological pathways associated with inflammation and cancer. The model also describes the dynamics of stem cell population in an inflammatory environment with respect to cell proliferation, differentiation, apoptosis, and the DNA damage responses that occur in single cells. The model incorporates cross-talk between the inflammatory microenvironment, and these cellular processes on different time scales ranging from the molecular kinetics of the DNA damage response (minutes to hours) and the individual cell cycle (~20 hours), to the protracted progression toward tumorigenesis, which may occur over a period of decades. Cell–cell interactions are not considered explicitly in the model, but enter through cell parameters that are dependent on population-level effects. Multiscale modeling lets us track and quantify the heterogeneity resulting from DNA damage and gene mutations in different cells. This heterogeneity plays an increasingly important role in theories of cancer stem cell evolution and has been intensively studied in the past decade. Moreover, our model provides a method that can be used to quantify the risk of inflammation-induced tumorigenesis based on both the degree and the duration of inflammation.

Model simulations conducted using the model predict biphasic dynamics on the route from inflammation to tumorigenesis. The two phases can be associated with the sequential accumulation of mutations in the pathways under consideration. Although mutations occur constantly in single cells in somatic tissues (35), only rare mutational events result in the accumulation of mutations leading to global changes in the cell. We classified mutations based on the biological pathways in which the genes within which they occur are involved and found that single mutations that affect the cell cycle–implicated pathways of proliferation, differentiation, and apoptosis were sufficient to induce abnormal cell growth. Following the occurrence of a precancerous state, when cells carrying a single mutation acquired a second mutation in a cell-cycle pathway or in the pathway of metabolism-immune balance, the tissue underwent increased abnormal growth, and tumorigenesis was initiated (Fig. 2A). The transition from the precancerous state to tumorigenesis was often associated with the emergence of double mutations (Fig. 3E). We identified possible dynamic biomarkers for the transition from the precancerous state to tumorigenesis; these include the occurrence of the double mutations, $\Delta Prolif^{+}\Delta Apop^{-}$, $\Delta Prolif^{+}\Delta Diff^{-}$, and $\Delta Prolif^{+}\Delta MIB^{-}$. These predictions complement recently identified dynamic biomarkers associated with cancer checkpoint blockade or critical transitions (36, 37), which have led to analysis of cell-to-cell variability through single-cell–based modeling (38, 39).

We have discovered multiple possible routes from inflammation to tumorigenesis. A mutation affecting the proliferation pathway $\Delta Prolif^{+}$ is the most prevalent first mutation in such routes; the other mutations considered ($\Delta Apop^{-}$, $\Delta Diff^{-}$ and ΔMIB^{-}) occur with approximately equal frequencies in subsequent events. Our model simulations corroborate the work of others in categorizing inflammation-induced tumorigenesis as a random process of multistage genomic changes (33, 40–43). It is a challenge to reconstruct the evolutionary history of a tumor based on genomic alterations. In our work, model simulations provide a way to explore different mutational routes toward tumorigenesis. We expect that further integration of cancer genomic data with this model will improve our ability to predict cancer development and patient survival (19). In the model, mutations to the pathways are represented as irreversible changes in the activities of the pathway. Biologically, changes to these parameters might also result from epigenetic modifications (44), and such changes may be reversible. The nature of how epigenetic control affects progression toward tumorigenesis remains open to further investigation.

Many patients with chronic inflammation display sustained mild inflammation but suffer occasional acute inflammation attacks. Our results showed that if the frequency of acute inflammation attacks was sufficiently low, these attacks usually did not increase the cancer risk. Long-term high frequency acute inflammation events can increase cancer risk (Fig. 5A). Most strikingly, this analysis revealed opposing effects of inflammation on tumorigenesis: sustained severe inflammation increases cancer risk due to an accumulation of DNA damage, but mild inflammation between acute inflammation attacks can attenuate the accumulation of DNA damage through the induction of damage-induced cell death and thus can decrease cancer risk. In particular, mild inflammation may trigger the elimination of DNA-damaged cells by the immune system.

In the model proposed here, the effects of microenvironment were represented through metabolism-immune balance–induced homeostasis. If we vary the level of inflammation and

Published OnlineFirst September 26, 2017; DOI: 10.1158/0008-5472.CAN-17-1662

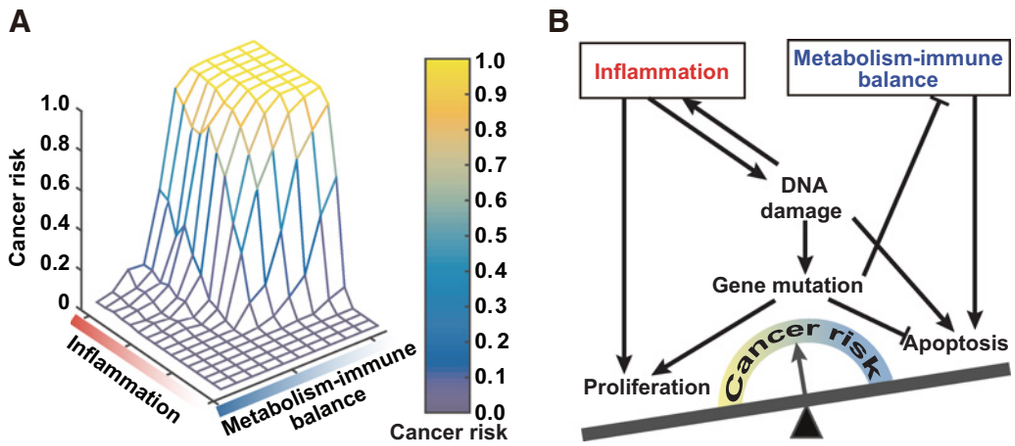

Figure 6.

Inflammation and cancer risk. **A,** Cancer risk as a function of varying values of inflammation ($0 < IS < 15$) and metabolism-immune balance ($0.01 > MIB > 0$). **B,** Summary of the role of inflammation and metabolism-immune balance in the regulation of cell regeneration. Inflammation promotes cell proliferation and DNA damage. DNA damage increases damage-induced cell death and promotes gene mutations that result in changes in the proliferation and apoptosis pathways. Metabolism-immune balance maintains system balance by triggering the immune response to remove mutant cells; however, the occurrence of gene mutations can upset this balance.

metabolism-immune balance, there is a sharp change from low to high cancer risk over a small parameter region (Fig. 6A). This sharp change suggests that there is a critical transition from low to high cancer risk. A balance between inflammation and the metabolism-immune response is thus crucial for a sustained low cancer risk; this balance is mediated by the competition between inflammation and the metabolism-immune balance response through the modulation of cell proliferation and death (Fig. 6B). This balance can be maintained under conditions of low-grade inflammation. However, under conditions of high-grade inflammation, the accumulation of DNA damages is capable of inducing cellular changes that perturb the metabolism-immune balance. Moreover, metabolism-immune imbalance can induce a series of abnormalities that ultimately lead to cancer (45). Thus, changes due to inflammation and metabolism-immune responses are important for the identification of biomarkers for inflammation-induced tumorigenesis and targets for therapeutic intervention. Although the appearance of a precancerous state can be markedly high in tissues (46–48), signals from the microenvironment are important for the persistence of this precancerous state. The current study highlights the fundamental role of signaling cross-talk between metabolism-immune balance and inflammatory control mechanisms.

Here, we sought to understand the progression from inflammation to tumorigenesis. The model we proposed is applicable to different types of cancers; however, the parameters may vary between different cancer types. Nevertheless, the qualitative conclusions reached in the current study are valuable for understanding the evolutionary dynamics of inflammation-induced cancer in various tissues. The computational model constructed here combined single-cell behavior with population dynamics. The biological processes represented in the model are essential for stem cell regeneration and are affected by the frequency of mutated genes in various cancers. The current model also serves as a springboard for other multiscale models of stem cell dynamics that can be used to discover the drivers of tumorigenesis. Other biological processes, such as the metabolism, the immune system, autophagy, telomere dynamics, and heterotypic cell responses to niche signals, could be added to extend the model further toward an integrative model of cancer development. Moreover, loss of homeostasis has been found to be closely related to cold syndrome and hot syndrome, which are key 1,000-year-old therapeutic concepts in traditional Chinese medicine and in particular manifest the metabolism-immune imbalance in patients with chronic atrophic gastritis (45, 49).

Cancer progression is an evolutionary process driven predominantly by somatic gene mutation and clonal cell expansion. Many of the elaborate regulatory circuits governing cancer progression have been discovered; however, predictive modeling of the evolutionary dynamics of cancer remains a key challenge for computational cancer biology (19). In this study, pertinent biological processes were represented through phenomenological parameters associated with their core pathways; the genetic details of their regulation were omitted. In particular, mutations were modeled via changes in the model parameters of certain pathways; they do not describe changes in specific genes. To investigate specific gene effects, an additional layer of complexity is required, that is, the gene-regulatory and epigenetic networks governing them (e.g., the networks involving NF-κB, APC, or TP53) should be included in the model. These additional details would allow us to link specific gene mutations to different phases of inflammation-induced tumorigenesis, an important step in understanding the network-driven mechanisms of complex diseases (50). By investigating the core pathways of cancer development through model simulation, such efforts will permit the discovery of promising new biomarkers and targets for the therapeutic prevention and treatment of inflammation-induced cancer.

Disclosure of Potential Conflicts of Interest

No potential conflicts of interest were disclosed.

Published OnlineFirst September 26, 2017; DOI: 10.1158/0008-5472.CAN-17-1662

Authors' Contributions

Conception and design: Q. Nie, Y. Li, J. Lei, S. Li
Development of methodology: Y. Guo, J. Lei, S. Li
Acquisition of data (provided animals, acquired and managed patients, provided facilities, etc.): S. Li
Analysis and interpretation of data (e.g., statistical analysis, biostatistics, computational analysis): Y. Guo, A.L. MacLean, J. Lei, S. Li
Writing, review, and/or revision of the manuscript: Y. Guo, Q. Nie, A.L. MacLean, J. Lei, S. Li
Administrative, technical, or material support (i.e., reporting or organizing data, constructing databases): J. Lei, S. Li
Study supervision: Q. Nie, Y. Li, J. Lei, S. Li

Grant Support

This study was supported in part by NSFC grants 91229201, 81630103, and 81225025 (to S. Li), NSFC grants 91430101 (to J. Lei), and NIH grants P50GM076516, R01GM107264, and R01NS095355, NSF grant DMS1562176, and a grant by Jayne Koskinas Ted Giovanis Foundation for Health and Policy joint with Breast Cancer Research Foundation (to Q. Nie).

The costs of publication of this article were defrayed in part by the payment of page charges. This article must therefore be hereby marked *advertisement* in accordance with 18 U.S.C. Section 1734 solely to indicate this fact.

Received June 5, 2017; revised August 3, 2017; accepted September 12, 2017; published OnlineFirst September 26, 2017.

References

1. Elinav E, Nowarski R, Thaiss CA, Hu B, Jin C, Flavell RA. Inflammation-induced cancer: crosstalk between tumours, immune cells and microorganisms. Nat Rev Cancer 2013;13:759–71.
2. Grivennikov SI, Greten FR, Karin M. Immunity, inflammation, and cancer. Cell 2010;140:883–99.
3. de Martel C, Ferlay J, Franceschi S, Vignat J, Bray F, Forman D, et al. Global burden of cancers attributable to infections in 2008: a review and synthetic analysis. Lancet Oncol 2012;13:607–15.
4. Parkin DM. The global health burden of infection-associated cancers in the year 2002. Int J Cancer 2006;118:3030–44.
5. Clevers H. At the crossroads of inflammation and cancer. Cell 2004;118:671–4.
6. Kuper H, Adami HO, Trichopoulos D. Infections as a major preventable cause of human cancer. J Intern Med 2000;248:171–83.
7. Lei J, Levin SA, Nie Q. Mathematical model of adult stem cell regeneration with cross-talk between genetic and epigenetic regulation. Proc Natl Acad Sci U S A 2014;111:E880–7.
8. Hanahan D, Weinberg RA. Hallmarks of cancer: the next generation. Cell 2011;144:646–74.
9. Kidane D, Chae WJ, Czochor J, Eckert KA, Glazer PM, Bothwell ALM, et al. Interplay between DNA repair and inflammation, and the link to cancer. Crit Rev Biochem Mol Biol 2014;49:116–39.
10. Licandro G, Ling Khor H, Beretta O, Lai J, Derks H, Laudisi F, et al. The NLRP3 inflammasome affects DNA damage responses after oxidative and genotoxic stress in dendritic cells. Eur J Immunol 2013;43:2126–37.
11. Moris D, Kontos M, Spartalis E, Fentiman IS. The role of NSAIDs in breast cancer prevention and relapse: current evidence and future perspectives. Breast Care 2016;11:339–44.
12. Yum H-W, Na H-K, Surh Y-J. Anti-inflammatory effects of docosahexaenoic acid: Implications for its cancer chemopreventive potential. Semin Cancer Biol 2016;40–41:141–59.
13. Zou K, Li Z, Zhang Y, Zhang H, Li B, Zhu W, et al. Advances in the study of berberine and its derivatives: a focus on anti-inflammatory and anti-tumor effects in the digestive system. Acta Pharmacol Sin 2017;38:157–67.
14. Ding Z, Liu S, Wang X, Khaidakov M, Dai Y, Mehta JL. Oxidant stress in mitochondrial DNA damage, autophagy and inflammation in atherosclerosis. Sci Rep 2013;3:1077.
15. Jaiswal M, LaRusso NF, Burgart LJ, Gores GJ. Inflammatory cytokines induce DNA damage and inhibit DNA repair in cholangiocarcinoma cells by a nitric oxide-dependent mechanism. Cancer Res 2000;60:184–90.
16. Thorsteinsdottir S, Gudjonsson T, Nielsen OH, Vainer B, Seidelin JB. Pathogenesis and biomarkers of carcinogenesis in ulcerative colitis. Nat Rev Gastroenterol Hepatol 2011;8:395–404.
17. Ziegler A, Koch A, Krockenberger K, Großhennig A. Personalized medicine using DNA biomarkers: a review. Humangenetik 2012;131:1627–38.
18. Altrock PM, Liu LL, Michor F. The mathematics of cancer: integrating quantitative models. Nat Rev Cancer 2015;15:730–45.
19. Beerenwinkel N, Greenman CD, Lagergren J. Computational cancer biology: an evolutionary perspective. Nussinov R, editor. PLoS Comput Biol 2016;12:e1004717.
20. Goodwin S, McPherson JD, McCombie WR. Coming of age: ten years of next-generation sequencing technologies. Nat Rev Genet 2016;17:333–51.
21. Anderson ARA, Quaranta V. Integrative mathematical oncology. Nat Rev Cancer 2008;8:227–34.
22. Byrne HM. Dissecting cancer through mathematics: from the cell to the animal model. Nat Rev Cancer 2010;10:221–30.
23. Poleszczuk J, Macklin P, Enderling H. Agent-based modeling of cancer stem cell driven solid tumor growth. Methods Mol Biol 2016;1516:335–46.
24. Scott JG, Fletcher AG, Anderson ARA, Maini PK. Spatial metrics of tumour vascular organisation predict radiation efficacy in a computational model. PLoS Comput Biol 2016;12:e1004712.
25. Lipkin M, Sherlock P, Bell B. Generation time of epithelial cells in the human colon. Nature 1962;195:175–7.
26. Menche J, Sharma A, Kitsak M, Ghiassian SD, Vidal M, Loscalzo J, et al. Uncovering disease-disease relationships through the incomplete interactome. Science 2015;347:1257601.
27. Meira LB, Bugni JM, Green SL, Lee C-W, Pang B, Borenshtein D, et al. DNA damage induced by chronic inflammation contributes to colon carcinogenesis in mice. J Clin Invest 2008;118:2516–25.
28. Eaden JA, Abrams KR, Mayberry JF. The risk of colorectal cancer in ulcerative colitis: a meta-analysis. Gut 2001;48:526–35.
29. Lynch M. Rate, molecular spectrum, and consequences of human mutation. Proc Natl Acad Sci U S A 2010;107:961–8.
30. Vineis P, Berwick M. The population dynamics of cancer: a Darwinian perspective. Int J Epidemiol 2006;35:1151–9.
31. Gerstung M, Baudis M, Moch H, Beerenwinkel N. Quantifying cancer progression with conjunctive Bayesian networks. Bioinformatics 2009;25:2809–15.
32. Rahnenführer J, Beerenwinkel N, Schulz WA, Hartmann C, von Deimling A, Wullich B, et al. Estimating cancer survival and clinical outcome based on genetic tumor progression scores. Bioinformatics 2005;21:2438–46.
33. Drost J, van Jaarsveld RH, Ponsioen B, Zimberlin C, van Boxtel R, Buijs A, et al. Sequential cancer mutations in cultured human intestinal stem cells. Nature 2015;521:43–7.
34. Hagemann T, Balkwill F, Lawrence T. Inflammation and cancer: a double-edged sword. Cancer Cell 2007;12:300–1.
35. Rossman TG, Goncharova EI, Nádas A. Modeling and measurement of the spontaneous mutation rate in mammalian cells. Mutat Res 1995;328:21–30.
36. Lesterhuis WJ, Bosco A, Millward MJ, Small M, Nowak AK, Lake RA. Dynamic versus static biomarkers in cancer immune checkpoint blockade: unravelling complexity. Nat Rev Drug Discov 2017;16:264–72.
37. Liu R, Wang X, Aihara K, Chen L. Early diagnosis of complex diseases by molecular biomarkers, network biomarkers, and dynamical network biomarkers. Med Res Rev 2014;34:455–78.
38. Mojtahedi M, Skupin A, Zhou J, Castaño IG, Leong-Quong RYY, Chang H, et al. Cell fate decision as high-dimensional critical state transition. PLoS Biol 2016;14:e2000640.
39. Richard A, Boullu L, Herbach U, Bonnafoux A, Morin V, Vallin E, et al. Single-cell-based analysis highlights a surge in cell-to-cell molecular variability preceding irreversible commitment in a differentiation process. PLoS Biol 2016;14:e1002585.
40. Frank SA. Dynamics of cancer: incidence, inheritance, and evolution. Princeton/Oxford, United Kingdom: Princeton University Press; 2007.
41. Gerstung M, Eriksson N, Lin J, Vogelstein B, Beerenwinkel N. The temporal order of genetic and pathway alterations in tumorigenesis. PLoS One 2011;6:e27136.

Published OnlineFirst September 26, 2017; DOI: 10.1158/0008-5472.CAN-17-1662

42. Tomasetti C, Marchionni L, Nowak MA, Parmigiani G, Vogelstein B. Only three driver gene mutations are required for the development of lung and colorectal cancers. Proc Natl Acad Sci U S A 2015;112:118–23.
43. Zhang X, Simon R. Estimating the number of rate limiting genomic changes for human breast cancer. Breast Cancer Res Treat 2005;91:121–4.
44. Hirsch P, Zhang Y, Tang R, Joulin V, Boutroux H, Pronier E, et al. Genetic hierarchy and temporal variegation in the clonal history of acute myeloid leukaemia. Nat Commun 2016;7:12475.
45. Li R, Ma T, Gu J, Liang X, Li S. Imbalanced network biomarkers for traditional Chinese medicine Syndrome in gastritis patients. Sci Rep 2013;3:1543.
46. Broström O, Löfberg R, Ost A, Reichard H. Cancer surveillance of patients with longstanding ulcerative colitis: a clinical, endoscopical, and histological study. Gut 1986;27:1408–13.
47. Lennard-Jones JE, Morson BC, Ritchie JK, Williams CB. Cancer surveillance in ulcerative colitis. Experience over 15 years. Lancet 1983;2:149–52.
48. Myrvold HE, Kock NG, Ahrén C. Rectal biopsy and precancer in ulcerative colitis. Gut 1974;15:301–4.
49. Li S, Zhang Z, Wu L, Zhang X, Li Y, Wang Y. Understanding ZHENG in traditional Chinese medicine in the context of neuro-endocrine-immune network. IET Syst Biol 2007;1:51–60.
50. Wu X, Jiang R, Zhang MQ, Li S. Network-based global inference of human disease genes. Mol Syst Biol 2008;4:189.

Published OnlineFirst September 26, 2017; DOI: 10.1158/0008-5472.CAN-17-1662

Cancer Research
The Journal of Cancer Research (1916–1930) | The American Journal of Cancer (1931–1940)

AACR American Association for Cancer Research

Multiscale Modeling of Inflammation-Induced Tumorigenesis Reveals Competing Oncogenic and Oncoprotective Roles for Inflammation

Yucheng Guo, Qing Nie, Adam L. MacLean, et al.

Cancer Res 2017;77:6429-6441. Published OnlineFirst September 26, 2017.